Novel functions of MDMX and innovative therapeutic strategies for melanoma

Heijkants, R.C.

CHAPTER 2

MDMX regulates transcriptional activity of p53 and FOXO

R.C. Heijkants[1], A.F.A.S Teunisse[1], D. de Jong[1], H. Mei[2], S. Kielbasa[2], K. Szuhai[1], A.G. Jochemsen[1].

1) Department of Cell and Chemical Biology, Leiden University Medical Center, Leiden, The Netherlands

2) Department of Biomedical Data Sciences, Leiden University Medical Center, Leiden, The Netherlands

Abstract

Tumor suppressor p53 has an important role in cell-fate determination. In cancer cells p53 activity is frequently inhibited by high levels of MDMX and/or MDM2. MDM2 is an E3 ubiquitin ligase whose activity results in ubiquitin- and proteasome-dependent p53 degradation, while MDMX shields p53's transactivation domain. Interestingly, the oncogenic functions of MDMX appear more wide-spread than exclusively the inhibition of p53. The present study sets out to elucidate the MDMX controlled transcriptome. Therefore, we depleted MDMX from a high MDMX expressing uveal melanoma cell line and determined the effect on the transcriptome by RNAseq. Biological function analyses indicate the inhibition of the cell cycle- and stimulation of cell death- regulating genes upon selective MDMX depletion. Although the inhibition of p53 activity clearly contributes to the transcription regulation controlled by MDMX, it appeared that the regulation of multiple genes did not fully rely on p53 expression. Analysis of gene regulatory networks suggests a role for Forkhead box (FOX) transcription factors. Indeed, an increased level of FOXO1 protein was observed upon MDMX depletion, independent of p53 expression. The mechanism of the p53-independent oncogenic functions of MDMX could be partially explained by these p53-independent effects on the transcriptome possibly regulated by FOXO1. As an example, we demonstrate that MXD4 (also named MAD4) expression is controlled by MDMX in a p53-independent manner. Interestingly, we found that MXD4 depletion activates p53 potentially suggesting a backup system in which MXD4 promotes MDM2 activity upon MDMX depletion. In order to enhance p53 activating strategies the MXD4 is proposed as a potential new therapeutic target.

Introduction

The p53 protein is considered to be a master regulator in a cell, mainly due to its central role in cellular stress sensing and its ability to regulate the transcription of a plethora of genes involved in multiple biological processes including cell cycle regulation, apoptosis, metabolism and autophagy [1]. Upon various types of intra- and extracellular stress p53 is activated and stabilized, resulting in transcriptional regulation inducing cell cycle arrest, senescence or apoptosis [2, 3]. Because of its central and important function in cell-fate, p53 activity needs to be under tight control. This stringent control of p53 is provided by many proteins including the ubiquitin E3 ligase MDM2 and the structurally related MDMX. This was best demonstrated *in vivo* were knock out of MDM2 or MDMX in mice resulted in embryonic lethality, which was shown to be p53-dependent [3-7]. Although both MDM2 and MDMX are crucial for mouse embryonic development, in adult tissue MDM2 loss is always lethal whereas MDMX often has more mild effects, indicative of the differences in expression and functions between the two proteins [8-14]. MDM2 is an E3 ubiquitin ligase and has been shown to directly bind with its N-terminal hydrophobic pocket to the N-terminal α helix of p53 and subsequently ubiquitinate p53, which consequently is sent for proteasomal degradation [15-18]. MDMX was initially discovered as a novel p53 interactor with high sequence homology and great structural similarities with MDM2 [19-21]. Despite the high conservation of the acidic domain and the RING domain MDMX does not have any E3 ubiquitin ligase activity. However, MDMX can, via its RING finger, form a heterodimer with MDM2, enhancing MDM2's ubiquitin ligase activity [22-24]. MDMX directly inhibits transcriptional activation by p53 by tightly binding and thereby shielding its transactivation domain [17, 18]. Considering that the levels of MDM2 and MDMX are crucial for the level and/or activity of p53 in a cell, also the levels of MDM2 and MDMX are under stringent control. Upon certain stress, e.g. DNA damage, p53 has to be liberated from its inhibitors MDM2 and MDMX. One mechanism is the degradation of both proteins by increased MDM2-mediated ubiquitination via decreased de-ubiquitination by ubiquitin specific protease (USP) 7 [5, 18, 25]. Additionally, serine-threonine kinase ATM-mediated phosphorylation on MDM2 inhibits its ubiquitin ligase activity towards p53 [26]. As a result the p53 protein is activated and stabilized and can perform its tumor suppressor function. During the recovery phase after an insult, a cell needs to re-constrain p53 activity by MDM2 and MDMX. It has been demonstrated that both MDM2 and MDMX are transcriptional targets of p53 providing a negative feedback loop [27, 28].

Approximately 50% of all human cancers contain a genetically altered p53 gene, either a point mutation or a deletion leading to loss of expression, to render cancer cells re-

sistant to the tumor suppressor function of p53 [29, 30]. Despite the high frequency of p53 mutations the other half of the human cancers evolved alternative mechanisms to attenuate p53 signaling [31]. Amplifications of MDM2 or MDMX are frequently found in sarcoma, glioblastoma, retinoblastoma and breast cancer, providing an interesting therapeutic target, i.e. re-activation of wild-type p53 by inhibition of MDM2/MDMX-p53 interaction [32]. Nutlin-3 was the first small molecule compound reported to exploit MDM2 overexpression by disrupting the MDM2 and p53 interaction resulting in stabilization of p53, subsequently inducing cell cycle arrest and apoptosis [33]. Importantly, it has been demonstrated that this p53 activation by Nutlin-3 was not due to activation of the DNA damage response [34, 35]. Recently it has been shown that the abundance of a naturally occurring MDMX short transcript isoform (MDMX-S) can be promoted using anti-sense oligonucleotides resulting in a shift from the full length to the short RNA isoform leading to decreased MDMX protein levels [36]. MDMX has been shown to be a potent therapeutic target in retinoblastoma, melanoma [37] and wild-type p53 breast cancer [38]. MDMX depletion induced cell cycle arrest and apoptosis in cancer cells in a partly p53-independent manner [37, 39], which could imply that MDMX is not only a valuable therapeutic target in wild-type p53 cancer cells, but also in p53 mutated cells. Indeed in p53 mutated breast cancer cell lines expressing high levels of MDMX protein the expression of MDMX was shown to be essential for cell viability and tumor growth [40]. This could be, at least partly, explained by the p53-independent upregulation of CDK inhibitory protein p27 upon MDMX depletion [39]. Furthermore, high levels of MDMX inhibit the early DNA damage response, independently of p53 and MDM2, resulting in genome instability [41]. However, the exact mechanisms leading to the p53 independent oncogenic functions of MDMX remain unspecified. Here we set out to elucidate to which extent the transcriptome is controlled by MDMX in a wild-type p53 cell line and how transcription regulation by MDMX might explain both its p53-dependent and -independent functions.

Results

Regulation of transcriptional activity by MDMX

The effect of p53 reactivation on the transcriptome has been studied extensively in previous studies (reviewed by: [42]). Here we studied the regulation of the transcriptome by MDMX. For this purpose we used a wild-type p53 cell line (MEL202) derived from a primary uveal melanoma, a cancer which rarely has mutated p53 and frequently highly express MDMX to constrain p53 activity [43]. We had shown before that this cell line is dependent on MDMX expression for proliferation [39]. We generated five MEL202-derived cell lines; one cell line containing a doxycycline-

inducible control shRNA expression construct and four cell lines containing a distinct doxycycline-inducible MDMX targeting shRNA expression construct.

Efficiency and kinetics of knockdown was tested by incubating the cells with doxycycline for 24, 48 and 72 hrs and harvesting both RNA and protein. These initial experiments show that the depletion of MDMX was efficient from 24 hours onwards with all shRNA constructs used (Figure 1A). Based on known p53 targets p21 and MAD2L1 we determined the transcriptional kinetics upon MDMX depletion (Figure 1B). The increase of CDK inhibitor p21 expression was already present at 24 hours and did not increase dramatically in the later time points. Mitotic arrest deficient 2 like 1 (MAD2L1), a component of the mitotic spindle assembly checkpoint, repression was only modest at 24, but reached plateau at 48 hours.

Based on these results we have performed transcriptional profiling by RNA sequencing upon doxycycline-inducible MDMX knockdown using 4 different shRNAs and 1 inducible control shRNA incubated with doxycycline for 48 hours. Thorough analysis of the data resulted in the identification of 176 genes which were significantly upregulated at least 0.7log2 fold upon MDMX depletion (Supplementary Table 1). Besides induction of expression, 70 genes were significantly down regulated with at least -0.7log2 fold upon MDMX depletion (Supplementary Table 2.). Gene ontology (GO) terms pathway analysis clearly showed that the upregulated genes promote cell death and apoptosis, while the down regulated genes are associated with genes involved in controlling the cell cycle (Supplementary Table 3).

To determine whether these effects are mediated via a specific transcription factor we employed the computational method iRegulon [44]. It turned out that of the 176 upregulated genes 66 have a p53 binding motive in their promotor regions (Supplementary Figure 1 and Supplementary Table 1) indicating that, despite the limited log fold changes, 37.5% of the upregulated genes could be explained by the p53 activation upon MDMX depletion. It appeared also from these analysis that the majority (114 of the 176, 65%) of the upregulated genes have a Forkhead Box (FOX) DNA binding motive, recognized by multiple FOX transcription factors. Interestingly, the genes containing a p53 DNA binding motive contained also a FOX motive in 89% of the cases. Analysis of the downregulated genes indicated enrichment for two known repressive transcription regulators, E2F4 and SIN3A. In total 61 of the 70 (87%) downregulated genes contained one or both repressive transcription regulators binding sites (Supplementary Figure 1 and Supplementary Table 2). We verified the transcriptional regulation of a number of these genes using qPCR (Figure 2A). Not only at the RNA level but also at protein level the upregulation of p21 (CDKN1A) and p53 upregulated

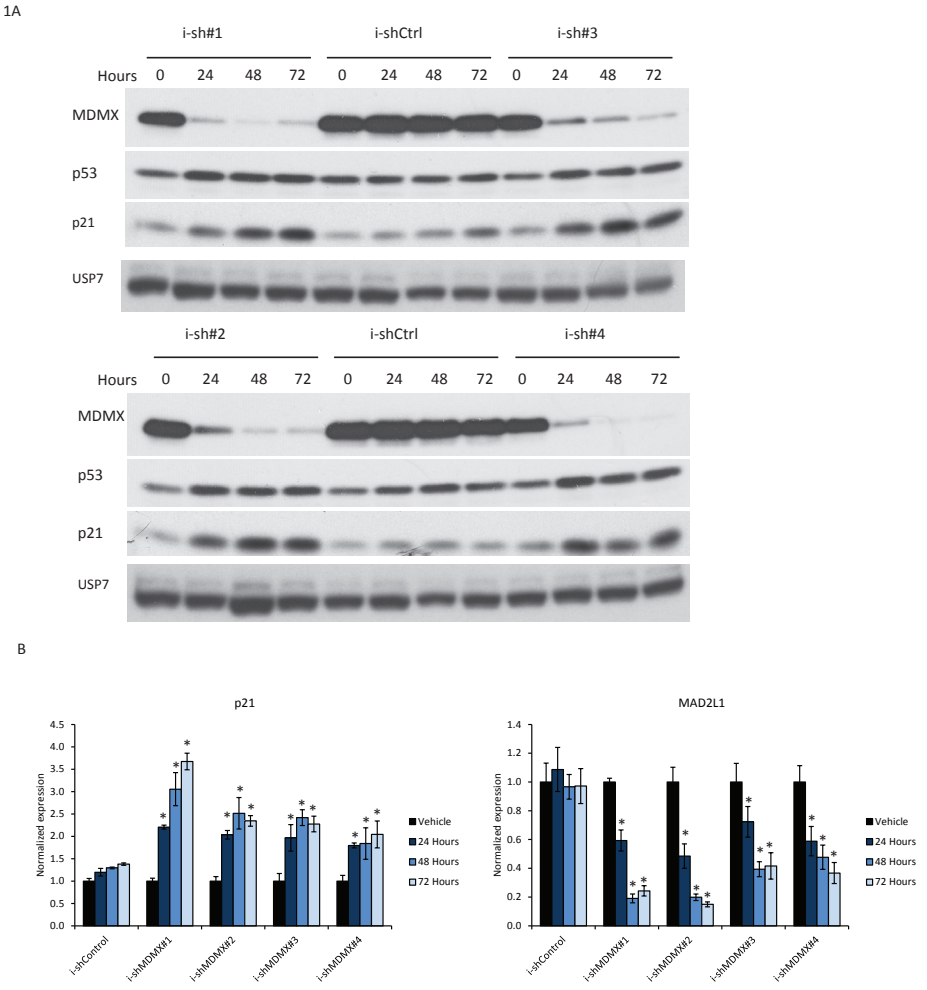

Figure 1. Kinetics of MDMX depletion in MEL202 cells upon doxycycline treatment. A) Protein expression analysis of i-shCtrl and i-shMDMX MEL202 cells harvested after different incubation periods with doxycycline. The cells containing the distinct MDMX targeting shRNA constructs (#1, 2, 3 and 4) show a clear reduction of MDMX protein upon doxycycline treatment (10 ng/ml). Simultaneously with MDMX depletion p53 levels slightly increase and also p21 levels rise, mostly at the later time points. B) Relative mRNA expression of p21 and MAD2L1 in i-shCtrl and i-shMDMX MEL202 cells harvested after different incubation periods with doxycycline (10 ng/ml). Expression of p21 is markedly increased upon MDMX depletion already after 24 hrs and only slightly increases at later time points. Repression of MAD2L1 upon MDMX depletion takes approximately 48 hours before reaching a plateau. Significant differences between the ish-Control and ish-MDMX knockdowns are indicated with an asterisk (*).

modulator of apoptosis (PUMA or BBC3) and downregulation of MAD2L1 could be confirmed (Figure 2B). Importantly, not only the sequence data was confirmed but also the expression of the transcription factors binding to the motives identified by iRegulon (p53 and FOXO1) were slightly increased upon MDMX depletion (Figure 2B). Importantly, both p53 and FOXO1 were found to interact with MDMX in MEL202 cells (Figure 2C). This interaction could be stabilized by the inhibition of the proteasome using MG132. Furthermore, the transcriptional regulation of the same down- and up-regulated MDMX target genes were also tested in a second uveal melanoma cell line (92.1) upon MDMX knockdown. In this cell line similar changes were observed as upon MDMX knockdown in MEL202 (Supplementary Figure 2A). These results indicate that the effects observed in the RNA sequencing are reliable and not cell line dependent.

p53-dependent and -independent effects

We and others have previously shown that depletion of MDMX can result in a p53-independent growth arrest. We, therefore, determined to what extend the observed MDMX induced effects on the transcriptome are p53-dependent. As an initial step we investigated whether non-genotoxic activation of p53 by Nutlin-3 would affect the expression of the same genes as observed upon MDMX depletion. As expected, we observed that the mRNA level of the known p53 target gene p21 (CDKN1A) is strongly induced upon Nutlin-3 treatment (Figure 2D). Similar effects were observed for cytoplasmic FMR1 interacting protein 2 (CYFIP2) and patched domain containing 4 (PTCHD4) (Figure 2C). Max dimerizing protein 4 (MXD4) and phosphoinositide-3-kinase interacting protein 1 (PIK3IP1) expression was also increased upon Nutlin-3 treatment, although the induction was much less compared to p21, CYFIP2 or PTCHD4. The mRNA levels of all genes downregulated upon MDMX knockdown that were tested (exonuclease 1 (EXO1), hyaluronan synthase 2(HAS2), kinesin family member 23 (KIF23), MAD2L1 and minichromosome maintenance 10 replication initiation factor (MCM10)) were also repressed upon incubation with Nutlin-3 (Figure 2D). To investigate a putative cell line dependency of the regulation of these genes by p53 we investigated the effect of Nutlin-3 treatment in another uveal and in four cutaneous melanoma cell lines, of which 94.07 contain a p53-inactivating mutation. Nutlin-3 treatment of the uveal melanoma cell line 92.1 showed transcriptional regulation of these genes similar to the results in MEL202 (Supplementary Figure 3). p53 wild type cutaneous melanoma cell lines 04.01 and 06.24 showed upon Nutlin-3 treatment that p21, CYFIP1 and PTCHD4 are potent p53 targets, whereas PIK3IP1 and MXD4 expression levels hardly, if anything, changed (Supplementary Figure 3). It can be noted that, although p21, CYFIP1, PTCHD4 responded in every cell line, the levels of increase vary significantly per cell line. Nutlin-3 treatment of both cutaneous melanoma lines resulted in a strong decrease of mRNA levels of genes downregulated upon MDMX

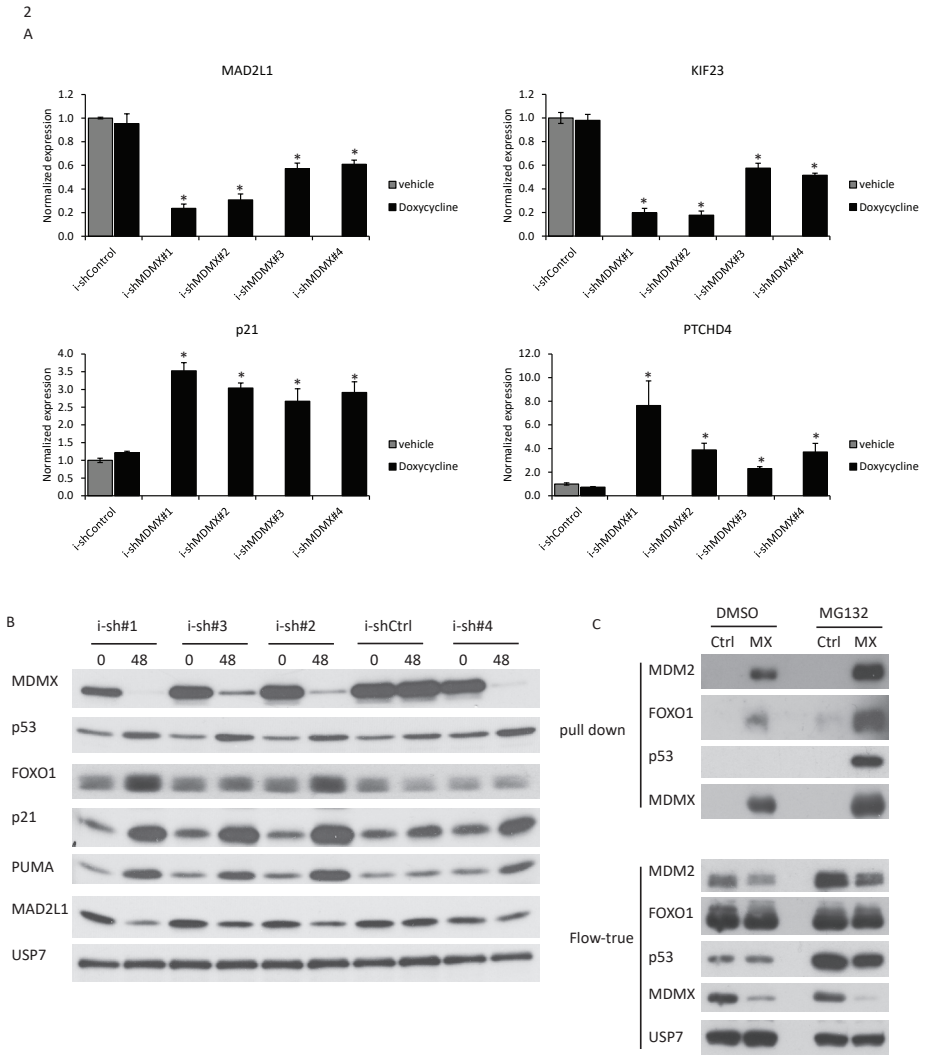

Figure 2. Verification of MDMX target genes. A) Relative Expression of MAD2L1, KIF23, p21 and PTCHD4 genes after 48 hours of doxycycline treatment of indicated cell lines. MAD2L1 and KIF23 are downregulated and p21 and PTCHD4 are upregulated upon MDMX knockdown. Significant differences in expression between doxycycline treated ish-Control cells and ish-MDMX cells is indicated with an asterisk (*). B) Analysis of protein expression after 48 hours doxycycline treatment shows a consistent repression of MAD2L1 level and an increase in p53, FOXO1, p21 and PUMA levels upon MDMX depletion. C) Pull-down of MDMX shows that both p53 and FOXO1 interact with MDMX. By inhibiting the proteasome, using MG132, this interaction is stabilized.

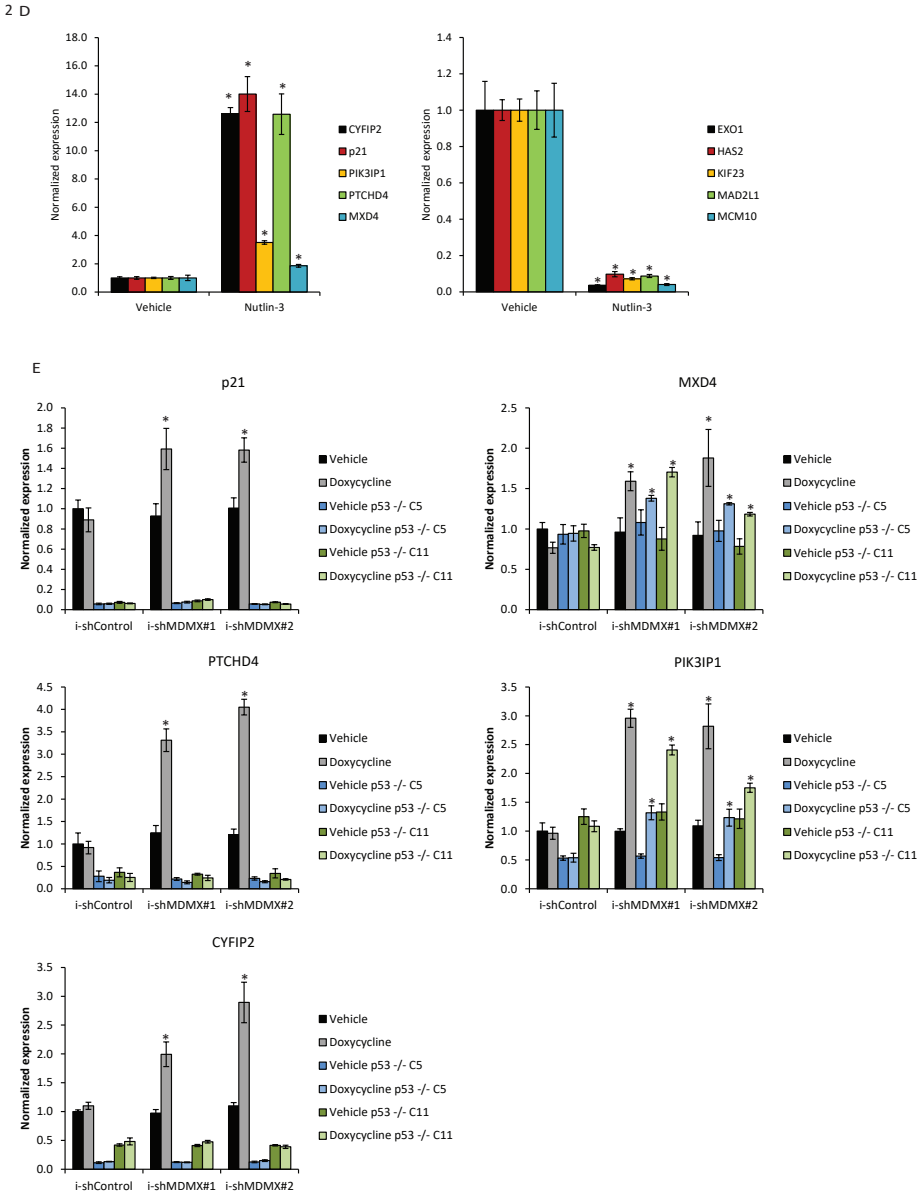

Figure 2. Verification of MDMX target genes. D) Relative mRNA expression of MDMX target genes in MEL202 cells upon 24 hour incubation with 4 µM Nutlin-3. Significant differences in gene expression between vehicle and Nutlin-3 are indicted with an asterisk (*). E) Relative mRNA expression of MDMX target genes upon MDMX depletion (48 hrs doxycycline, 10 ng/ml) in both MEL202 wild-type and MEL202 p53 knockout cells. Gene expression which was significantly up-regulated upon MDMX depletion is indicated with an asterisk (*).

depletion, except for HAS2; some transcriptional repression of HAS2 could only be found 06.24 (Supplementary Figure 3). Cutaneous melanoma cell line 94.07 has an inactivating mutation in p53, which indeed coincides with limited observed changes in the mRNA levels of the analysed genes upon Nutlin-3 treatment (Supplementary Figure 3). Together these results demonstrate that the p53 targets found upon MDMX knockdown are indeed bona fide p53 targets in melanoma in general.

As a second step to study the p53-dependency of the changes in the transcriptome upon MDMX depletion, we created MEL202 cells deficient of p53 using CRISPR/CAS9 technology) [45, 46]. We selected two clones which fully lack any detectable p53 protein as a consequence of an adenine insertion (after nucleotide position 143 of the coding sequence) resulting in the mutation of ASP48 to GLU and simultaneously introducing an alternative reading frame resulting in an early translation stop after amino acid position 50 (Supplementary Figure 4A and B). This lack of p53 protein renders the cells, as expected, resistant for Nutlin-3 induced growth arrest (Supplementary Figure 4C). The p53 KO cells did not show any aberrations in their karyotype at chromosomal level compared with the parental cell line as determined by combined binary ratio fluorescence in situ hybridization (COBRA FISH) (Supplementary Figure 4D). From these cells doxycycline-inducible shMDMX or -inducible shCtrl cell lines were generated. With the use of these cell lines we could clearly demonstrate that the increased expression of p21, PTCHD4 and CYFIP2 upon MDMX depletion is fully p53-dependent (Figure 2E). Interestingly, also the basal levels of these genes are largely p53-dependent, indicating that there is some basal p53 activity in these cells. Although both PIK3IP1 and MXD4 were found to be direct p53 targets genes according to our iRegulon analysis, upon MDMX depletion the expression of both genes was increased independently of p53 expression (Figure 2E). Although the MDMX depletion triggered induction of these genes is p53-independent, the Nutlin-3 mediated increase of both MXD4 and PIK3IP1 expression occurred p53-dependent (Supplementary figure 5A), even though the basal levels of both PIK3IP1 and MXD4 were not affected by p53 knockout. We again analysed 92.1 cells to confirm these data, albeit with shp53/mediated p53 depletion instead of knock out. Also in these cells the expression of p21, PTCHD4 and CYFIP2 was found to be p53-dependently upregulated upon MDMX depletion, but increased expression of PIK3IP1 and MXD4 is p53-independent (Supplementary Figure 2A and B). IRegulon network analysis further indicated the involvement of FOXOs in the transcriptional changes upon MDMX depletion. The previous mentioned upregulation of FOXO1 was indeed found to be p53-independent (supplementary figure 5B). These data show that not all upregulated genes upon MDMX depletion are p53 target genes in these cell lines, possibly explaining the p53-independent growth stimulatory functions of MDMX.

Similarly, we found that in both MEL202 and 92.1 cell lines the transcriptional repression of genes upon MDMX knockdown in many cases is partially, but not fully dependent on p53 expression (Supplementary Figure 2A and Supplementary Figure 6).

MXD4 in uveal melanoma

To study the p53-independent functions of MDMX in greater detail we focussed on MXD4, which according to previous studies forms a transcription repressive complex with SIN3A. It has also previously been shown that SIN3A can interact with and protect p53 from MDM2 mediated ubiquitination and degradation [47, 48]. We hypothesized that upregulation of MXD4 upon MDMX depletion could function as a 'rescue' mechanism for the tumor cell to counteract the p53 activation. We propose a model in which the increased MXD4 levels sequester a proportion of SIN3A and thereby partly liberate p53 for MDM2-mediated ubiquitination resulting in its degradation. Supporting this model is our finding that MXD4 knockdown in MEL202 induced a p53-dependent growth arrest, indicating a p53 activating effect (Figure 3A and B). This suggestion is strengthened by the observation that the p53 target gene p21 is upregulated in MXD4 knockdown cells. Similarly, the p53 repressed genes MAD2L1 and KIF23 are slightly downregulated in MXD4 knockdown cells (Figure 3A). Interestingly, these effects on p53 target genes could be further enhanced by MDMX knockdown. As expected, these enhanced transcriptional effects correlated with a stronger growth reduction in a long term cell proliferation assay (Figure 3C).

To investigate whether MXD4 knockdown also boosts other p53 stabilizing and/or activating approaches, cells were treated with a low dose of Nutlin-3 (MDM2/X inhibitor), doxorubicin (topoisomerase 2 inhibitor) or XI-011 (inducer of MDMX depletion). In a three day cell viability assay neither MXD4 knockdown nor drug treatments had a strong effect on cell survival. However, the combination of MXD4 knockdown with either Nutlin-3, doxorubicin or XI-011 showed a synergistic reduction in cell survival (Figure 4A). These effects mostly correlate with an enhanced cell cycle arrest upon doxorubicin or XI-011 treatment (G1 and G2/M, respectively) (Figure 4B and C). Neither MXD4 knockdown nor the low concentration drug treatment affected MDMX levels, but did slightly increase p53 levels (Figure 4B). In accordance with the enhanced biological effects, the MXD4 knockdown increases the induction of PUMA by Nutlin-3 and XI-011, and the p21 induction by doxorubicin and XI-011 treatment. Likewise, MAD2L1 repression seems to be slightly more prominent in the MXD4 knockdown cells.

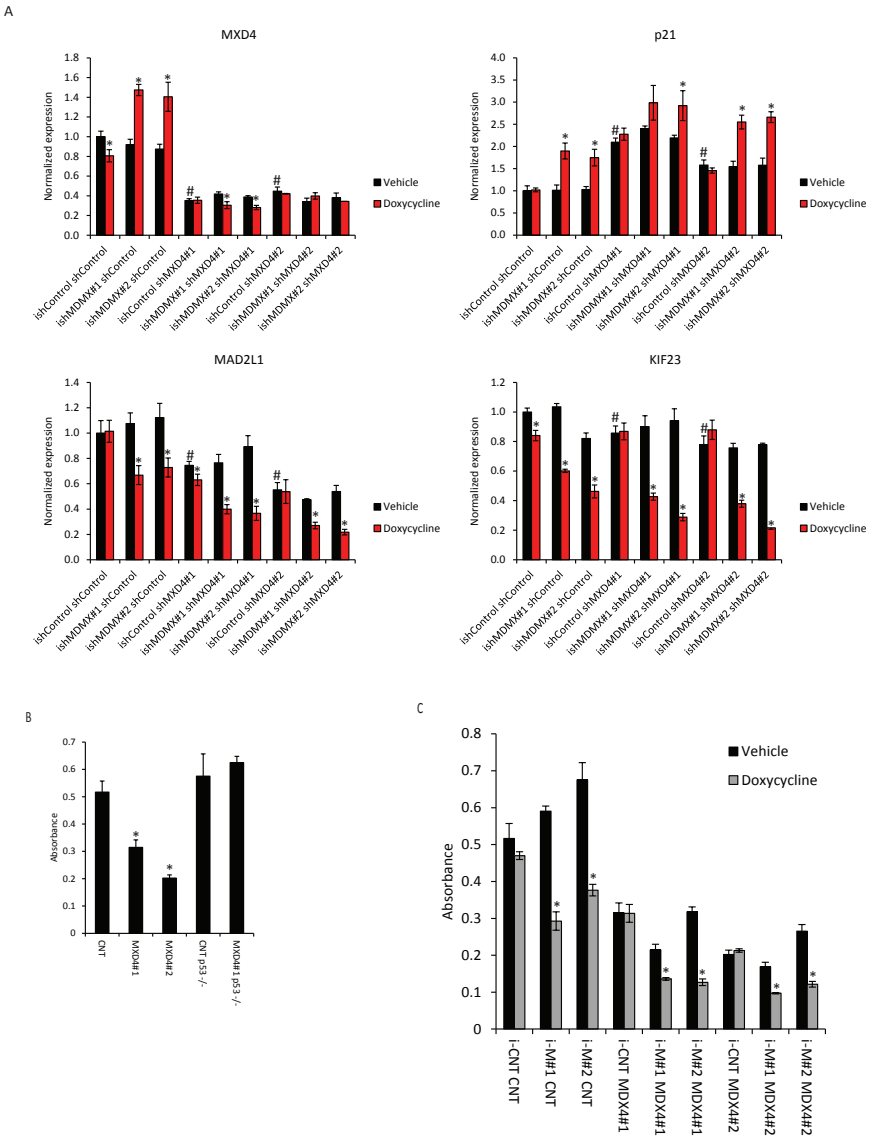

Figure 3. MXD4 knockdown activates p53, inhibits cell growth and enhances effect of MDMX knockdown in MEL202 cells. Relative mRNA expression of MXD4, p21, MAD2L1, PIK3IP1 and KIF23 upon MDMX knockdown in sh-Control and sh-MXD4 cells. Asterisk (*) indicates significant differences between vehicle and doxycycline treated cell line. Significant differences in normalized expression between sh-Control and shMXD4 targeting constructs in cells expressing ish-Control are indicated with a hashtag (#). B) Quantification of long term growth assay of MEL202 MXD4 knockdown cells in p53 wildtype and p53 knockout cells and C) MEL202 cells with either MXD4, MDMX or combined knockdown. Significant differences in absorbance between Control and sh-MXD4 (B) and between vehicle and doxycycline treated (C) is indicated with an asterisk (*).

Discussion

Our studies presented here make it evident that MDMX is affecting the transcription of genes which are implicated in cell cycle regulation and apoptosis. Further analysis of the downregulated MDMX target genes indicate that E2F4- and SIN3A-mediated transcription repression is involved. To discriminate whether SIN3A or E2F4 is essential for the repression of these target genes will be essentially impossible. First, because it has been shown that in SIN3A knock out cells E2F target genes are regulated [49] and, secondly, because previous studies actually showed that SIN3A forms a repressive complex with E2F4 [50, 51]. Most likely a large repressive complex is formed, containing multiple transcription repressive factors like HDACs, to ensure proper target gene repression.

Based on large meta-analysis performed by Fisher and colleagues our results suggest that depletion of MDMX liberates p53, resulting in increased levels of p21 protein, which in turn leads to the activation of the DP, RB-like, E2F4 and Muvb (DREAM) complex, resulting in the repression of target genes [52-54]. Of the 210 essential regulators of G2 phase and mitosis assigned to be regulated by the p53-p21-DREAM axis [53], we identify 23 genes down regulated upon MDMX depletion. The identification of the p53-p21-E2F4/SIN3A axis for 87% of the repressed genes seems to indicate that MDMX controls the transcriptional activity of p53 to control cell cycle progression. However, MDMX clearly has (wt)-p53 independent oncogenic functions [37, 39-41]. Such a p53-independent biological function could correlate with our observation that in distinct cell lines the repression of target genes upon MDMX depletion is not fully p53 dependent. It suggests that MDMX depletion is triggering E2F4/SIN3A-mediated target gene repression that is in part independent of p53.

The list of upregulated genes upon MDMX knockdown contains 66 genes that are potentially regulated directly by p53 of which multiple genes are among the most commonly found p53 activated genes, namely CDKN1A, zinc finger matrin-type 3 (ZMAT3), tumor protein p53 inducible nuclear protein 1 (TP53INP1), tetraspanin 11 (TSPAN11), ectodysplasin a2 receptor (EDA2R) and CYFIP2 [42], indicating that p53 transactivation is repressed by MDMX in our uveal melanoma cells as expected. Surprisingly, although the regulation of most verified genes identified as p53 targets upon MDMX depletion is highly dependent on p53 expression, the regulation of at least PIK3IP1 and MXD4 is not. Both genes were identified as p53-responsive genes in previous studies, but since a clear p53 DNA binding near the promoter region could not be found they were not assigned as true p53 target gene status [52]. Also in our hands the responsiveness of these genes to p53 activation upon Nutlin-3 treatment

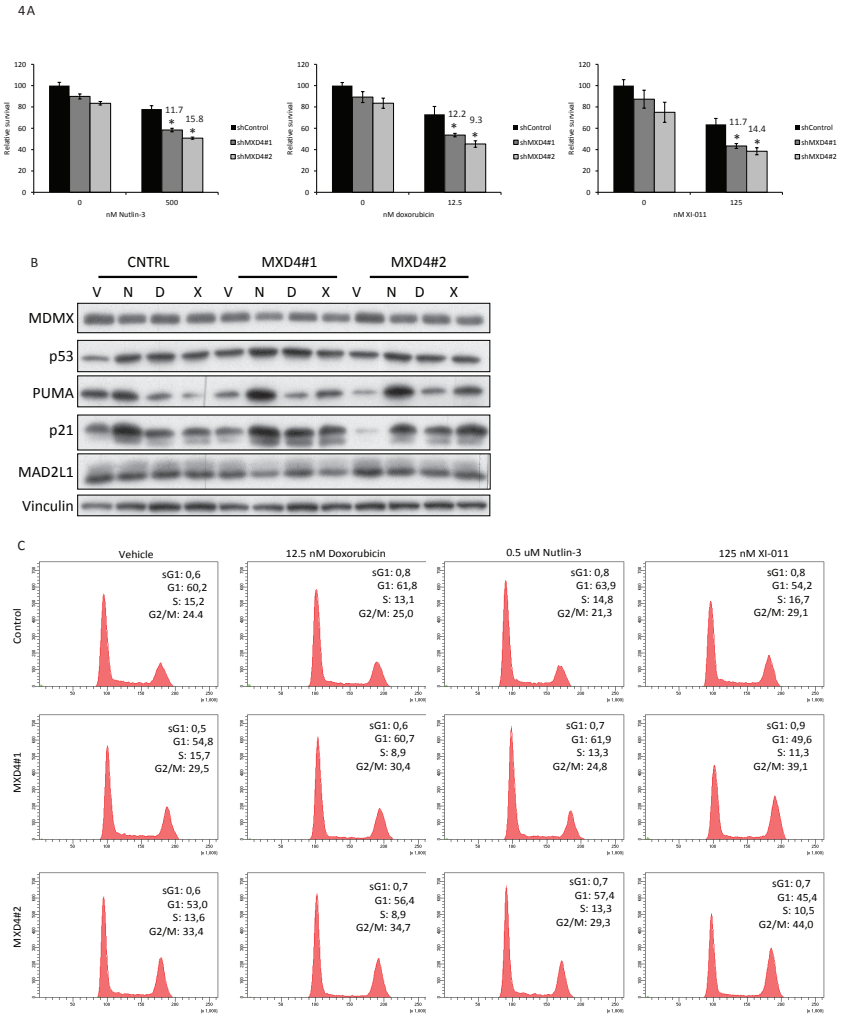

Figure 4. MXD4 knockdown sensitizes cells for p53 activation. A) Relative survival of MEL202 sh-Ctrl and shMXD4 cells treated for 72 hrs with 0.5 µM Nutlin-3 (N), 12.5 nM Doxorubicin (D), 125 nM XI-011 (X) or vehicle (V). Numbers indicate the Excess over Bliss scores of the combination treated samples. An asterisk (*) indicates significant differences in relative survival comparing the combination treatment with both single treatments. Scores above 2.0 indicate synergism. B) Protein expression analysis of the cells treated as mentioned in A. While MDMX and p53 protein levels hardly change upon combination treatments compared to single treatment, levels of downstream p53 targets p21, PUMA and to a lesser extent MAD2L1 show a stronger response in the combination treated samples. Vinculine expression was assessed to show equal loading. C) Cell cycle profiles of cells treated as indicated at A. Doxorubicin-treated cells show an enhanced S-phase depletion when combined with MXD4 knockdown, while the profiles of the combined MXD4 knockdown + Nutlin-3 treated samples show intermediate phenotype compared to single treatments. Cells with combined MXD4 knockdown and XI-011 showed a clearly enhanced G2/M arrest.

is very weak. Interestingly, both PIK3IP1 and MXD4 contain, like 65% of all the up-regulated genes upon MDMX depletion, FOX transcription factor DNA binding sites. PIK3IP1 has been demonstrated to be a direct FOXO3 target [55]. We could verify that FOXO1 is stabilized upon MDMX depletion in a p53-independent manner. It could be hypothesized that MDMX, by the demonstrated binding of FOXO1, inhibits FOXO1 explaining, at least partly, the p53-independent oncogenic functions of MDMX.

The MXD4 (MAD4) protein has been described as an antagonist for c-MYC by competing with c-MYC for MAX dimerization [56-58]. Possibly relevant for our story is the observation that MXD4 is not only a c-MYC antagonist, but it can also form a transcriptional repressor complex with SIN3A [59]. SIN3A has also been reported to bind p53 and thereby protect it from MDM2-mediated ubiquitination and degradation [47, 48]. Since the reduced proliferation upon MXD4 knockdown is p53-dependent, we hypothesize that MXD4 can repress p53 activity by binding SIN3A, allowing enhanced MDM2-mediated degradation of p53. Indeed we observed a small increase in p53 protein level upon MXD4 knockdown, suggesting that MXD4 is involved in p53 stability. In addition, various p53 stabilizing and activating strategies could be enhanced upon MXD4 knockdown, i.e. upon MDMX depletion, MDM2/X inhibition via Nutlin-3, and treatment of the cells with doxorubicin or XI-011.

In conclusion, our data presented here suggest the existence a novel back-up loop in which a FOX transcription factor is released or activated upon MDMX depletion resulting in increased MXD4 expression. Subsequently, MXD4 competes with p53 for SIN3A binding, sensitizing p53 for MDM2-mediated degradation thereby blunting the p53 tumor suppressor response. Implicating that MXD4 is a potential novel target to boost current p53 activating strategies.

Acknowledgements

The authors like to acknowledge Prof S. van de Burg and Dr. E. Verdegaal for the kind donation of cell lines 94.07 04.01, 04.04 and 06.24. The authors like to acknowledge Dr. M. Goncalves for his assistance and the kind donation of the adenoviral expression vectors used during the establishment of p53 knockout cells.

References

1. Bieging KT, Mello SS, Attardi LD. Unravelling mechanisms of p53-mediated tumour suppression. Nat Rev Cancer. 2014; 14: 359-70. doi: 10.1038/nrc3711.
2. Riley T, Sontag E, Chen P, Levine A. Transcriptional control of human p53-regulated genes. Nat Rev Mol Cell Biol. 2008; 9: 402-12. doi: 10.1038/nrm2395.
3. Jones SN, Roe AE, Donehower LA, Bradley A. Rescue of embryonic lethality in Mdm2-deficient mice by absence of p53. Nature. 1995; 378: 206-8. doi: 10.1038/378206a0.
4. Montes de Oca Luna R, Wagner DS, Lozano G. Rescue of early embryonic lethality in mdm2-deficient mice by deletion of p53. Nature. 1995; 378: 203-6. doi: 10.1038/378203a0.
5. Okamoto K, Kashima K, Pereg Y, Ishida M, Yamazaki S, Nota A, Teunisse A, Migliorini D, Kitabayashi I, Marine JC, Prives C, Shiloh Y, Jochemsen AG, et al. DNA damage-induced phosphorylation of MdmX at serine 367 activates p53 by targeting MdmX for Mdm2-dependent degradation. Mol Cell Biol. 2005; 25: 9608-20. doi: 10.1128/MCB.25.21.9608-9620.2005.
6. Finch RA, Donoviel DB, Potter D, Shi M, Fan A, Freed DD, Wang CY, Zambrowicz BP, Ramirez-Solis R, Sands AT, Zhang N. mdmx is a negative regulator of p53 activity in vivo. Cancer Res. 2002; 62: 3221-5. doi:
7. Parant J, Chavez-Reyes A, Little NA, Yan W, Reinke V, Jochemsen AG, Lozano G. Rescue of embryonic lethality in Mdm4-null mice by loss of Trp53 suggests a nonoverlapping pathway with MDM2 to regulate p53. Nat Genet. 2001; 29: 92-5. doi: 10.1038/ng714.
8. Francoz S, Froment P, Bogaerts S, De Clercq S, Maetens M, Doumont G, Bellefroid E, Marine JC. Mdm4 and Mdm2 cooperate to inhibit p53 activity in proliferating and quiescent cells in vivo. Proc Natl Acad Sci U S A. 2006; 103: 3232-7. doi: 10.1073/pnas.0508476103.
9. Marine JC, Francoz S, Maetens M, Wahl G, Toledo F, Lozano G. Keeping p53 in check: essential and synergistic functions of Mdm2 and Mdm4. Cell Death Differ. 2006; 13: 927-34. doi: 10.1038/sj.cdd.4401912.
10. Valentin-Vega YA, Okano H, Lozano G. The intestinal epithelium compensates for p53-mediated cell death and guarantees organismal survival. Cell Death Differ. 2008; 15: 1772-81. doi: 10.1038/cdd.2008.109.
11. Valentin-Vega YA, Box N, Terzian T, Lozano G. Mdm4 loss in the intestinal epithelium leads to compartmentalized cell death but no tissue abnormalities. Differentiation. 2009; 77: 442-9. doi: 10.1016/j.diff.2009.03.001.
12. Grier JD, Xiong S, Elizondo-Fraire AC, Parant JM, Lozano G. Tissue-specific differences of p53 inhibition by Mdm2 and Mdm4. Mol Cell Biol. 2006; 26: 192-8. doi: 10.1128/MCB.26.1.192-198.2006.
13. Ringshausen I, O'Shea CC, Finch AJ, Swigart LB, Evan GI. Mdm2 is critically and continuously required to suppress lethal p53 activity in vivo. Cancer Cell. 2006; 10: 501-14. doi: 10.1016/j.ccr.2006.10.010.
14. Moyer SM, Larsson CA, Lozano G. Mdm proteins: critical regulators of embry ogenesis and homeostasis. J Mol Cell Biol. 2017. doi: 10.1093/jmcb/mjx004.
15. Barak Y, Oren M. Enhanced binding of a 95 kDa protein to p53 in cells undergoing p53-mediated growth arrest. EMBO J. 1992; 11: 2115-21. doi:
16. Momand J, Zambetti GP, Olson DC, George D, Levine AJ. The mdm-2 oncogene product forms a complex with the p53 protein and inhibits p53-mediated transactivation. Cell. 1992; 69: 1237-45. doi:
17. Kawai H, Wiederschain D, Yuan ZM. Critical contribution of the MDM2 acidic domain to p53 ubiquitination. Mol Cell Biol. 2003; 23: 4939-47. doi:
18. Meulmeester E, Frenk R, Stad R, de Graaf P, Marine JC, Vousden KH, Jochemsen AG. Critical role for a central part of Mdm2 in the ubiquitylation of p53. Mol Cell Biol. 2003; 23: 4929-38. doi:

19. Shvarts A, Steegenga WT, Riteco N, van Laar T, Dekker P, Bazuine M, van Ham RC, van der Houven van Oordt W, Hateboer G, van der Eb AJ, Jochemsen AG. MDMX: a novel p53-binding protein with some functional properties of MDM2. EMBO J. 1996; 15: 5349-57. doi:
20. Marine JC, Jochemsen AG. Mdmx and Mdm2: brothers in arms? Cell Cycle. 2004; 3: 900-4. doi:
21. Bottger V, Bottger A, Garcia-Echeverria C, Ramos YF, van der Eb AJ, Jochemsen AG, Lane DP. Comparative study of the p53-mdm2 and p53-MDMX interfaces. Oncogene. 1999; 18: 189-99. doi: 10.1038/sj.onc.1202281.
22. Sharp DA, Kratowicz SA, Sank MJ, George DL. Stabilization of the MDM2 oncoprotein by interaction with the structurally related MDMX protein. J Biol Chem. 1999; 274: 38189-96. doi:
23. Gu J, Kawai H, Nie L, Kitao H, Wiederschain D, Jochemsen AG, Parant J, Lozano G, Yuan ZM. Mutual dependence of MDM2 and MDMX in their functional inactivation of p53. J Biol Chem. 2002; 277: 19251-4. doi: 10.1074/jbc.C200150200.
24. Linares LK, Hengstermann A, Ciechanover A, Muller S, Scheffner M. HdmX stimulates Hdm2-mediated ubiquitination and degradation of p53. Proc Natl Acad Sci U S A. 2003; 100: 12009-14. doi: 10.1073/pnas.2030930100.
25. Pereg Y, Shkedy D, de Graaf P, Meulmeester E, Edelson-Averbukh M, Salek M, Biton S, Teunisse AF, Lehmann WD, Jochemsen AG, Shiloh Y. Phosphorylation of Hdmx mediates its Hdm2- and ATM-dependent degradation in response to DNA damage. Proc Natl Acad Sci U S A. 2005; 102: 5056-61. doi: 10.1073/pnas.0408595102.
26. Stommel JM, Wahl GM. Accelerated MDM2 auto-degradation induced by DNA-damage kinases is required for p53 activation. EMBO J. 2004; 23: 1547-56. doi: 10.1038/sj.emboj.7600145.
27. Phillips A, Teunisse A, Lam S, Lodder K, Darley M, Emaduddin M, Wolf A, Richter J, de Lange J, Verlaan-de Vries M, Lenos K, Bohnke A, Bartel F, et al. HDMX-L is expressed from a functional p53-responsive promoter in the first intron of the HDMX gene and participates in an autoregulatory feedback loop to control p53 activity. J Biol Chem. 2010; 285: 29111-27. doi: 10.1074/jbc.M110.129726.
28. Pigolotti S, Krishna S, Jensen MH. Oscillation patterns in negative feedback loops. Proc Natl Acad Sci U S A. 2007; 104: 6533-7. doi: 10.1073/pnas.0610759104.
29. Hollstein M, Hergenhahn M, Yang Q, Bartsch H, Wang ZQ, Hainaut P. New approaches to understanding p53 gene tumor mutation spectra. Mutat Res. 1999; 431: 199-209. doi:
30. Hainaut P, Hollstein M. p53 and human cancer: the first ten thousand mutations. Adv Cancer Res. 2000; 77: 81-137. doi:
31. Vogelstein B, Lane D, Levine AJ. Surfing the p53 network. Nature. 2000; 408: 307-10. doi: 10.1038/35042675.
32. Gao J, Aksoy BA, Dogrusoz U, Dresdner G, Gross B, Sumer SO, Sun Y, Jacobsen A, Sinha R, Larsson E, Cerami E, Sander C, Schultz N. Integrative analysis of complex cancer genomics and clinical profiles using the cBioPortal. Sci Signal. 2013; 6: pl1. doi: 10.1126/scisignal.2004088.
33. Vassilev LT, Vu BT, Graves B, Carvajal D, Podlaski F, Filipovic Z, Kong N, Kammlott U, Lukacs C, Klein C, Fotouhi N, Liu EA. In vivo activation of the p53 pathway by small-molecule antagonists of MDM2. Science. 2004; 303: 844-8. doi: 10.1126/science.1092472.
34. Vassilev LT. MDM2 inhibitors for cancer therapy. Trends Mol Med. 2007; 13: 23-31. doi: 10.1016/j.molmed.2006.11.002.
35. de Lange J, Ly LV, Lodder K, Verlaan-de Vries M, Teunisse AF, Jager MJ, Jochemsen AG. Synergistic growth inhibition based on small-molecule p53 activation as treatment for intraocular melanoma. Oncogene. 2012; 31: 1105-16. doi: 10.1038/onc.2011.309.

36. Dewaele M, Tabaglio T, Willekens K, Bezzi M, Teo SX, Low DH, Koh CM, Rambow F, Fiers M, Rogiers A, Radaelli E, Al-Haddawi M, Tan SY, et al. Antisense oligonucleotide-mediated MDM4 exon 6 skipping impairs tumor growth. J Clin Invest. 2016; 126: 68-84. doi: 10.1172/JCI82534.
37. Gembarska A, Luciani F, Fedele C, Russell EA, Dewaele M, Villar S, Zwolinska A, Haupt S, de Lange J, Yip D, Goydos J, Haigh JJ, Haupt Y, et al. MDM4 is a key therapeutic target in cutaneous melanoma. Nat Med. 2012; 18: 1239-47. doi: 10.1038/nm.2863.
38. Haupt S, Buckley D, Pang JM, Panimaya J, Paul PJ, Gamell C, Takano EA, Lee YY, Hiddingh S, Rogers TM, Teunisse AF, Herold MJ, Marine JC, et al. Targeting Mdmx to treat breast cancers with wild-type p53. Cell Death Dis. 2015; 6: e1821. doi: 10.1038/cddis.2015.173.
39. de Lange J, Teunisse AF, Vries MV, Lodder K, Lam S, Luyten GP, Bernal F, Jager MJ, Jochemsen AG. High levels of Hdmx promote cell growth in a subset of uveal melanomas. Am J Cancer Res. 2012; 2: 492-507. doi:
40. Jeffreena Miranda P, Buckley D, Raghu D, Pang JB, Takano EA, Vijayakumaran R, Teunisse AF, Posner A, Procter T, Herold MJ, Gamell C, Marine JC, Fox SB, et al. MDM4 is a rational target for treating breast cancers with mutant p53. J Pathol. 2017. doi: 10.1002/path.4877.
41. Carrillo AM, Bouska A, Arrate MP, Eischen CM. Mdmx promotes genomic instability independent of p53 and Mdm2. Oncogene. 2015; 34: 846-56. doi: 10.1038/onc.2014.27.
42. Fischer M. Census and evaluation of p53 target genes. Oncogene. 2017; 36: 3943-56. doi: 10.1038/onc.2016.502.
43. Jochemsen AG. Reactivation of p53 as therapeutic intervention for malignant melanoma. Curr Opin Oncol. 2014; 26: 114-9. doi: 10.1097/CCO.0000000000000033.
44. Janky R, Verfaillie A, Imrichova H, Van de Sande B, Standaert L, Christiaens V, Hulselmans G, Herten K, Naval Sanchez M, Potier D, Svetlichnyy D, Kalender Atak Z, Fiers M, et al. iRegulon: from a gene list to a gene regulatory network using large motif and track collections. PLoS Comput Biol. 2014; 10: e1003731. doi: 10.1371/journal.pcbi.1003731.
45. Maggio I, Stefanucci L, Janssen JM, Liu J, Chen X, Mouly V, Goncalves MA. Selection-free gene repair after adenoviral vector transduction of designer nucleases: rescue of dystrophin synthesis in DMD muscle cell populations. Nucleic Acids Res. 2016; 44: 1449-70. doi: 10.1093/nar/gkv1540.
46. Holkers M, Maggio I, Henriques SF, Janssen JM, Cathomen T, Goncalves MA. Adenoviral vector DNA for accurate genome editing with engineered nucleases. Nat Methods. 2014; 11: 1051-7. doi: 10.1038/nmeth.3075.
47. Murphy M, Ahn J, Walker KK, Hoffman WH, Evans RM, Levine AJ, George DL. Transcriptional repression by wild-type p53 utilizes histone deacetylases, mediated by interaction with mSin3a. Genes Dev. 1999; 13: 2490-501. doi:
48. Zilfou JT, Hoffman WH, Sank M, George DL, Murphy M. The corepressor mSin3a interacts with the proline-rich domain of p53 and protects p53 from proteasome-mediated degradation. Mol Cell Biol. 2001; 21: 3974-85. doi: 10.1128/MCB.21.12.3974-3985.2001.
49. McDonel P, Demmers J, Tan DW, Watt F, Hendrich BD. Sin3a is essential for the genome integrity and viability of pluripotent cells. Dev Biol. 2012; 363: 62-73. doi: 10.1016/j.ydbio.2011.12.019.
50. Dannenberg JH, David G, Zhong S, van der Torre J, Wong WH, Depinho RA. mSin3A corepressor regulates diverse transcriptional networks governing normal and neoplastic growth and survival. Genes Dev. 2005; 19: 1581-95. doi: 10.1101/gad.1286905.
51. Li H, Collado M, Villasante A, Matheu A, Lynch CJ, Canamero M, Rizzoti K, Carneiro C, Martinez G, Vidal A, Lovell-Badge R, Serrano M. p27(Kip1) directly represses Sox2 during embryonic stem cell differentiation. Cell Stem Cell. 2012; 11: 845-52. doi: 10.1016/j.stem.2012.09.014.

52. Fischer M, Grossmann P, Padi M, DeCaprio JA. Integration of TP53, DREAM, MMB-FOXM1 and RB-E2F target gene analyses identifies cell cycle gene regulatory networks. Nucleic Acids Res. 2016; 44: 6070-86. doi: 10.1093/nar/gkw523.
53. Fischer M, Quaas M, Steiner L, Engeland K. The p53-p21-DREAM-CDE/CHR pathway regulates G2/M cell cycle genes. Nucleic Acids Res. 2016; 44: 164-74. doi: 10.1093/nar/gkv927.
54. Fischer M, Steiner L, Engeland K. The transcription factor p53: not a repressor, solely an activator. Cell Cycle. 2014; 13: 3037-58. doi: 10.4161/15384101.2014.949083.
55. Schmidt-Strassburger U, Schips TG, Maier HJ, Kloiber K, Mannella F, Braunstein KE, Holzmann K, Ushmorov A, Liebau S, Boeckers TM, Wirth T. Expression of constitutively active FoxO3 in murine forebrain leads to a loss of neural progenitors. FASEB J. 2012; 26: 4990-5001. doi: 10.1096/fj.12-208587.
56. Grinberg AV, Hu CD, Kerppola TK. Visualization of Myc/Max/Mad family dimers and the competition for dimerization in living cells. Mol Cell Biol. 2004; 24: 4294-308. doi:
57. Hurlin PJ, Queva C, Koskinen PJ, Steingrimsson E, Ayer DE, Copeland NG, Jenkins NA, Eisenman RN. Mad3 and Mad4: novel Max-interacting transcriptional repressors that suppress c-myc dependent transformation and are expressed during neural and epidermal differentiation. EMBO J. 1996; 15: 2030. doi:
58. Rottmann S, Luscher B. The Mad side of the Max network: antagonizing the function of Myc and more. Curr Top Microbiol Immunol. 2006; 302: 63-122. doi:
59. Yang W, Yang X, David G, Dorsey JF. Dissecting the complex regulation of Mad4 in glioblastoma multiforme cells. Cancer Biol Ther. 2012; 13: 1339-48. doi: 10.4161/cbt.21814.
60. Chen PW, Murray TG, Uno T, Salgaller ML, Reddy R, Ksander BR. Expression of MAGE genes in ocular melanoma during progression from primary to metastatic disease. Clin Exp Metastasis. 1997; 15: 509-18. doi:
61. De Waard-Siebinga I, Blom DJ, Griffioen M, Schrier PI, Hoogendoorn E, Beverstock G, Danen EH, Jager MJ. Establishment and characterization of an uveal-melanoma cell line. Int J Cancer. 1995; 62: 155-61. doi:
62. Amirouchene-Angelozzi N, Frisch-Dit-Leitz E, Carita G, Dahmani A, Raymondie C, Liot G, Gentien D, Nemati F, Decaudin D, Roman-Roman S, Schoumacher M. The mTOR inhibitor Everolimus synergizes with the PI3K inhibitor GDC0941 to enhance anti-tumor efficacy in uveal melanoma. Oncotarget. 2016; 7: 23633-46. doi: 10.18632/oncotarget.8054.
63. Herold MJ, van den Brandt J, Seibler J, Reichardt HM. Inducible and reversible gene silencing by stable integration of an shRNA-encoding lentivirus in transgenic rats. Proc Natl Acad Sci U S A. 2008; 105: 18507-12. doi: 10.1073/pnas.0806213105.
64. Carlotti F, Bazuine M, Kekarainen T, Seppen J, Pognonec P, Maassen JA, Hoeben RC. Lentiviral vectors efficiently transduce quiescent mature 3T3-L1 adipocytes. Mol Ther. 2004; 9: 209-17. doi: 10.1016/j.ymthe.2003.11.021.
65. Chen X, Rinsma M, Janssen JM, Liu J, Maggio I, Goncalves MA. Probing the impact of chromatin conformation on genome editing tools. Nucleic Acids Res. 2016; 44: 6482-92. doi: 10.1093/nar/gkw524.
66. Szuhai K, Bezrookove V, Wiegant J, Vrolijk J, Dirks RW, Rosenberg C, Raap AK, Tanke HJ. Simultaneous molecular karyotyping and mapping of viral DNA integration sites by 25-color COBRA-FISH. Genes Chromosomes Cancer. 2000; 28: 92-7. doi:
67. Szuhai K, Tanke HJ. COBRA: combined binary ratio labeling of nucleic-acid probes for multi-color fluorescence in situ hybridization karyotyping. Nat Protoc. 2006; 1: 264-75. doi: 10.1038/nprot.2006.41.
68. Hof PV, Arindrarto W, Bollen S, Kielbasa S, Laros J, Mei H. (2017). BIOPET: Towards Scalable, Maintainable, User-Friendly, Robust and Flexible NGS Data Analysis Pipelines. 2017 17th IEEE/ACM International Symposium on Cluster, Cloud and Grid Computing (CCGRID), pp. 823-9.

Methods

Cell culture and viability assays

The UM cell lines MEL202 [60] and 92.1 [61] were cultured in a mixture of RPMI and DMEM-F12 (1:1 ratio), supplemented with 10% fetal calf serum (FCS) and antibiotics. Cutaneous melanoma lines 94.07 04.01, 04.04 and 06.24 were cultured in DMEM medium, supplemented with 10% FCS and antibiotics.

For short term growth assay the cells were seeded in triplicate, in 96-well format and incubated for 3 days with drugs as indicated. Cell survival was determined via the Cell Titre-Blue Cell Viability assay (Promega, Fitchburg, WI, USA); fluorescence was measured in a microplate reader (Victor, Perkin Elmer, San Jose, CA, USA). Excess over Bliss values were calculated to determine the synergism between two conditions as described by Amirouchene-Angelozzi N *et al.*[62].

For colony assays the cells were seeded in triplicate in 12-well plates and were incubated for 8 days. Cells were fixed for 5 minutes in 4% paraformaldehyde. DNA was stained using 30-minute incubation with 0.05% crystal violet. After washing and drying the relative number of cells was quantified by solubilizing the crystal violet in methanol and measuring absorbance at 545nM using a microplate reader (Victor3, Perkin Elmer).

Manipulation of cell lines

1. Establishment of inducible MDMX knockdown cell lines

Inducible shRNA knockdown lentiviral vectors were constructed as described previously [38, 63]. Production of lentivirus stocks by transfections into HEK293T cells essentially as described, but calcium phosphate was replaced with PEI [64]. Virus was quantitated by antigen capture ELISA measuring HIV p24 levels (ZeptoMetrix Corp., New York, NY, USA). Cells were transduced using MOI 2 in medium containing 8 µg/ml polybrene. Target sequences of shRNA constructs to deplete MDMX are: #1: 5'-GTGCAGAGGAAAGTTCCAC, #2: 5'- GAATCTCTTGAAGCCATGT, #3: 5'- CAGTCCTTCAGCTATTTCAT and #4: 5'- AGTCAAGACCAACTGAAGC. As a control shRNA the construct targeting 5'-GAATCTTGTTACATCAGCT was used.

2. Generation of p53 knockout MEL202-derived cells

MEL202 cells were transduced with puromycin-selectable lentiviral guideRNA expression construct (AA19_pLKO.1-puro.U6.sgRNA.Bvel-stuffer) [65], with targets the sequence: 5'-CCATTGTTCAATATCGTCCG-3' in exon 4 of the p53 gene. After selection on puromycin, Cas9 was temporarily expressed upon transduction with adenoviral

Cas9 expression construct ($AdV^{D2}P.Cas9.F^{50}$ [45]) or a control EGFP encoding adenoviral vector (20 IUs/cell). The EGFP-encoding adenoviral vector used differs from AdV.Δ2.$donor^{S1/T\text{-}TS}$ [46] in that it has FRT sites flanking an expression cassette consisting of the human PGK1 gene promoter, the EGFP ORF and the bovine growth hormone polyadenylation signal. Cells were selected for p53 inactivity by continuous presence of 4 μM of Nutlin-3 (Cayman Chemical, Ann Arbor, MI, USA) after which single cell derived clones were established and p53 protein expression was analyzed. To determine the exact mutation genomic DNA of these clones was isolated which was used as a template for PCR (Fw primer: GAGACCTGTGGGAAGCGAAA and Rv-primer: GCTGCCCTGGTAGGTTTTCT), followed by Sanger sequencing using the forward primer. To investigate chromosomal abnormalities upon CRISPR/Cas9-mediated p53 knockout, karyotyping of the cell lines was performed by COBRA-FISH as described earlier [66, 67].

RNA sequencing

MEL202 cells with 4 MDMX targeting doxycycline inducible shRNA constructs and 1 control shRNA construct were treated for 48 hours with 10 ng/ml doxycycline; the cell line containing the control shRNA construct was also mock treated to investigate doxycycline induced effects.

RNA was isolated from three independent biological replicates. RNA was isolated using miRNeasy (Qiagen, Hilden, Germany) and treated with DNAse (Qiagen) according to manufactures protocol. The quality of the samples was determined using a Bioanalyzer 6000 nanochip (Agilent), followed by ribosomalRNA depletion using Ribo-Zero (Epicentre, Madison, WI, USA) after which the libraries were constructed as described by the NEBNext Ultra Directional RNA Library Prep Kit for Illumina (NEB E7420S). Samples were pooled and sequenced on the HiSeq2500, run type paired-end 2x50bp + dual index on v4 reagents and flowcells. Read counts were extracted from the BAM files with FeatureCounts (version 1.5.3).

All RNAseq files were processed using the BIOPET Gentrap pipeline version 0.7 developed at the LUMC [68]. This pipeline performs FASTQ pre-processing (including quality control, quality trimming and adapter clipping), RNAseq alignment, read and base quantification, and optionally transcript assembly. In this project, FastQC version 0.11.2 was used for checking raw read QC. Low quality read trimming was done using Sickle version 1.33 with default settings. Adapter clipping was performed using Cutadapt version 1.9.1 with default settings. The RNAseq reads alignment was performed using GSNAP version 2014-12-23 with setting "--npaths 1 --quiet-if-excessive". The reference genome used was GRCh38 without the alternative contigs. The gene

read quantification was performed using HTSeq-count version 0.6.1p1 with setting "--stranded=reverse". The gene annotations used for quantification were GENCODE version 23.

For statistical analysis of the read counts R (version 3.4.2) was used. Read counts were normalized using quantile normalization in the DeSeq package (Version 1.16.1). Differential expression analysis was performed with DeSeq. Gene regulatory network analysis was performed using iRegulon (44). Enriched biological processes (GO) were determined using String-DB version 10.5.

RNA isolation, cDNA synthesis and real-time quantitative PCR

RNA was isolated using the SV total RNA isolation kit (Promega), after which the reverse transcriptase reaction mixture as indicated by Promega was used to synthesize cDNA. qPCR was performed using SYBR green mix (Roche Diagnostics, Indianapolis, IN, USA) in a C1000 touch Thermal Cycler (Bio-Rad laboratories, Hercules, CA, USA). Relative expression of target genes was determined in three independent experiments compared to housekeeping genes CAPNS1 and SRPR. Per experiment the average relative expression was compared to the untreated set at 1. For primer sequences see supplementary table 4.

Western blot analysis

After incubation with drugs as indicated cells were harvested in Laemmli sample buffer. SDS-PAGE was used to separate equal amounts of protein which were blotted onto polyvinylidene fluoride transfer membranes (Millipore, Darmstadt, Germany). Followed by blocking in TBST (10 mM Tris-HCl pH8.0, 150 mM NaCl, 0.2% Tween 20) containing 10% milk. Membranes were incubated with the proper primary antibodies: USP7 (A300-033A, Bethyl Laboratories, Montgomery, TX, USA), MDMX (8C6, Millipore, Burlington, MA, USA), p53 (DO1, Santa Cruz Biotechnology, Dallas, TX, USA), p21 (CP74, Millipore), PUMA (G3, Santa Cruz Biotechnology), MDM2 (SMP14, Santa Cruz Biotechnology; 3G9, Millipore), MAD2L1 (C2C3, Genetex, Irving, CA, USA) or Vinculin (hVIN-1/V9131, Sigma-Aldrich, St Louis, MO, USA)) and appropriate HRP-conjugated secondary antibodies (Jackson Laboratories, Bar Harbor, ME, USA). Chemoluminescence was used to visualize bands by exposure to X-ray film.

Flow cytometry

Cells were harvested for cell cycle analysis by trypsinization, washed twice in PBS and fixed in ice cold 70% ethanol. Following fixation, cells were washed in PBS containing 2% FCS and stained using PBS containing 2% FCS, 50 µg/ml RNAse and 50 µg/ml

propidium iodide (PI). Flow cytometry analysis was performed using the BD LSR II system (BD Biosciences, San Diego, CA, USA).

Immuno-precipitations

MEL202 cells, 80-90% confluent, were incubated with 10 µM MG132 for 5 hours to establish inhibition of the proteasome. Cells were washed twice with cold PBS and subsequently lyzed in a low salt containing Giordano buffer (50mM Tris-HCl pH7.4, 150 mM NaCl, 0.1% Triton X-100 and 5 mM EDTA; supplemented with phosphatase- and protease inhibitors and 15% glycerol). 500 µg of lysate was incubated with 30 µl of 50% bead suspension of HDMX or control beads (Chromotek, Planegg-Martinsried, Germany) in a final volume of 800 µl, tumbling for 16 hours at 4°C. After this incubation flow-through was collected. Beads were washed 3 times in lysis buffer according to manufactures instructions. Samples were eluted in 40 µl Laemmli buffer, incubated at 98°C for 5 minutes. Samples were span through a 0.2 µm nylon centrifugal filter (VWR, Radnor, PA, USA) to remove beads, elution's and flow-through (30 µl with 15 µl 3x Laemmli buffer incubated for 5 minutes at 98°C)were separated using SDS-PAGE and analysed as described above (Western blot analysis). Primary antibodies used for protein detection were C29H4 (Cell Signaling technology, Danvers, MA, USA) for FOXO1, a mix of SMP14 (Santa Cruz Biotechnology) and 3G9 (Millipore) was used for MDM2, DO1 (Santa Cruz Biotechnology) for p53, flow-through MDMX was detected using 8C6 (Millipore) and pull-down MDMX using MDMX-BL (Bethyl Laboratories). USP7 (A300-033A, Bethyl Laboratories) was detected to ensure equal loading of the flow-through.

Statistical analysis

Student's t-test was used to calculate the significance between two groups. P-values of 0.05 or less were considered to be significant.

Supplementary table 1. Upregulated genes upon MDMX knockdown

Gene ID	Log2FoldChange	iRegulon motive	
PTCHD4	1.92		
PIK3IP1	1.59	FOX	
CYFIP2	1.58	FOX	p53
ACTA2	1.57		
CDKN1A	1.48	FOX	p53
EDA2R	1.47	FOX	
MIR34A	1.45		
C10orf10	1.35	FOX	
BTG2	1.35		
TSPAN11	1.34	FOX	p53
PTGER4	1.23	FOX	p53
C10orf54	1.14	FOX	p53
ZMAT3	1.13	FOX	p53
MXD4	1.09	FOX	p53
FAM212B	1.09		
COL16A1	1.08	FOX	p53
CCDC18-AS1	1.07		
PLN	1.05	FOX	
FOXN3-AS1	1.05		
DDIT4	1.04	FOX	p53
p53INP1	1.04	FOX	
TCP11L2	1.02	FOX	p53
TXNIP	1.01	FOX	
MYO15B	1.00		
DENND2A	1.00	FOX	
PNRC1	0.99	FOX	
MIR100HG	0.98		
DHX58	0.98		
SORBS2	0.97	FOX	p53
ADAM19	0.95	FOX	
ADAMTS6	0.95	FOX	p53
COL24A1	0.95	FOX	
TAP1	0.95		
ERBB4	0.94	FOX	
YPEL2	0.94	FOX	p53
FOXP2	0.94	FOX	p53

Supplementary table 1. Upregulated genes upon MDMX knockdown (continued)

Gene ID	Log2FoldChange	iRegulon motive	
GAPDHP33	0.93		
RPS27L	0.93	FOX	p53
ARRDC3	0.93	FOX	p53
CASP4	0.93		
EFNA1	0.93	FOX	p53
AP1G2	0.92	FOX	p53
IL1RAPL1	0.92	FOX	
p53TG1	0.92		
PDGFC	0.92	FOX	
RASGRF2	0.92	FOX	
FILIP1	0.91	FOX	p53
FZD4	0.91	FOX	p53
SULF2	0.90	FOX	p53
TM7SF2	0.90		
SYTL2	0.90	FOX	
CFAP70	0.90		
L1CAM	0.89		
PHLDA3	0.89	FOX	p53
CFI	0.89		
LINC00518	0.89		
PLSCR4	0.88	FOX	
CTSO	0.88	FOX	
PPP1R9A	0.87	FOX	
S100B	0.87		
FEZ1	0.87	FOX	
NINJ1	0.86	FOX	p53
CDC42EP5	0.86	FOX	p53
P2RX6	0.86		
BTBD19	0.86		
JMY	0.85	FOX	
WDR66	0.85		
ADAMTS10	0.85	FOX	
LTBP4	0.85	FOX	
EPAS1	0.85		
GMPR	0.85	FOX	
KCNIP4-IT1	0.84		

Supplementary table 1. Upregulated genes upon MDMX knockdown (continued)

Gene ID	Log2FoldChange	iRegulon motive	
ITGB8	0.84	FOX	
KLHL30	0.84	FOX	
ALDH3B1	0.84	FOX	p53
DNASE1L1	0.84		
DRAM1	0.84		
FDXR	0.84	FOX	
JUN	0.84	FOX	
SATB1	0.84	FOX	p53
OPRL1	0.84	FOX	
DMD	0.83	FOX	p53
LACC1	0.83		
ABCA9	0.83	FOX	
RPS6KA2	0.82	FOX	
FSIP2	0.82		
FN1	0.82		
ABCA1	0.82	FOX	
RIMS2	0.82	FOX	p53
HSPB7	0.81	FOX	
C15orf52	0.81		p53
PLA2G4C	0.81		
PLK3	0.81	FOX	
MAML3	0.81	FOX	p53
ZNF630	0.81		
SFRP4	0.80		
PRSS23	0.80	FOX	p53
TSC22D1	0.80	FOX	
BBC3	0.80	FOX	p53
SESN1	0.80	FOX	p53
RND3	0.80	FOX	
MCF2L	0.80	FOX	p53
PCDHGA12	0.80		
SATB1-AS1	0.79		
SEMA3B	0.79	FOX	p53
ICAM5	0.79		
SLC4A3	0.78		p53
MDM2	0.78	FOX	p53

Supplementary table 1. Upregulated genes upon MDMX knockdown (continued)

Gene ID	Log2FoldChange	iRegulon motive	
March2	0.78		
ADAMTS13	0.78	FOX	
GADD45A	0.78	FOX	p53
ARSG	0.78	FOX	p53
C1RL	0.78		
PSMG3-AS1	0.78		
CALCOCO1	0.78		
KLF9	0.78	FOX	
ZNF610	0.77	FOX	
FAM214A	0.77		
KIF26B	0.77	FOX	
C1orf101	0.77	FOX	
LRRTM4	0.76	FOX	
ICA1	0.76	FOX	p53
GPR155	0.76	FOX	p53
RAB7B	0.76		
CUBN	0.76	FOX	
FHDC1	0.75	FOX	p53
DDB2	0.75		p53
LINC00346	0.75		
DOCK8	0.75		
JAG1	0.75	FOX	p53
ZRANB2-AS2	0.75		
SEMA6C	0.75	FOX	p53
ZNF536	0.75	FOX	
FBXO32	0.75	FOX	p53
FAM43A	0.75	FOX	
KLHL7-AS1	0.74		
ACER2	0.74		p53
ETFBKMT	0.74		
CD226	0.74	FOX	p53
PCDHA9	0.74		
DCLK1	0.74	FOX	
VPS37D	0.74		p53
DOK6	0.74	FOX	p53
EPHA2	0.74		p53

Supplementary table 1. Upregulated genes upon MDMX knockdown (continued)

Gene ID	Log2FoldChange	iRegulon motive	
NPAS3	0.73	FOX	
RHOJ	0.73	FOX	p53
LCA5L	0.73	FOX	
PBX1	0.73	FOX	
C1S	0.73		
CA8	0.73	FOX	
ITGAX	0.73		
PARD3B	0.73	FOX	p53
PBXIP1	0.72	FOX	
CNTN1	0.72	FOX	p53
NDRG1	0.72	FOX	
ASTN2	0.72	FOX	p53
HTR2B	0.72	FOX	p53
PLD1	0.72	FOX	p53
LRRC37A3	0.72	FOX	
PLK2	0.72		p53
LAMA4	0.72	FOX	
PQLC3	0.72		
ITGA3	0.71	FOX	p53
COL4A5	0.71	FOX	
GDPD1	0.71		
SV2B	0.71		
FAM227A	0.71		
C1orf116	0.71	FOX	p53
RCAN2	0.71	FOX	
EHHADH	0.71	FOX	p53
ZNF528	0.71		
FAP	0.71	FOX	p53
CRIM1	0.71	FOX	p53
LIMA1	0.70	FOX	p53
IGFBP7	0.70	FOX	p53
RRM2B	0.70	FOX	p53

Supplementary table 2. Downregulated genes upon MDMX knockdown

Gene ID	Log2FoldChange	iRegulon motive	
CEP128	-1.54		
LMNB1	-0.93	E2F4	SIN3A
KIF14	-0.93	E2F4	SIN3A
HLX	-0.92	E2F4	
IDH1	-0.90	E2F4	SIN3A
DTL	-0.88	E2F4	SIN3A
ANP32E	-0.87	E2F4	SIN3A
KIF4B	-0.87		
HAS2	-0.87	E2F4	
MTFR2	-0.87		
SCML1	-0.87	E2F4	
AURKB	-0.86	E2F4	SIN3A
CENPI	-0.85	E2F4	SIN3A
DCLRE1A	-0.85	E2F4	SIN3A
MDM4	-0.83	E2F4	
CDC25A	-0.83		SIN3A
AUNIP	-0.82		
SKA3	-0.81	E2F4	SIN3A
SPAG5	-0.80		SIN3A
KIF23	-0.80		SIN3A
SUV39H1	-0.79	E2F4	SIN3A
CHAF1A	-0.79	E2F4	SIN3A
ERCC6L	-0.79	E2F4	SIN3A
BRCA1	-0.78	E2F4	SIN3A
MCM7	-0.78	E2F4	SIN3A
MAD2L1	-0.78		SIN3A
MCM10	-0.78	E2F4	SIN3A
NUF2	-0.77	E2F4	SIN3A
WDR62	-0.77	E2F4	SIN3A
NMRK2	-0.77		
PBK	-0.77	E2F4	SIN3A
MCM3	-0.77		SIN3A
WDR76	-0.77	E2F4	SIN3A
SASS6	-0.76	E2F4	SIN3A
GSG2	-0.76		SIN3A

Supplementary table 2. Downregulated genes upon MDMX knockdown (continued)

Gene ID	Log2FoldChange	iRegulon motive	
CHAF1B	-0.76	E2F4	
ZNF114	-0.75		
CLSPN	-0.75	E2F4	SIN3A
FKBP5	-0.75	E2F4	SIN3A
MCM4	-0.75	E2F4	SIN3A
SKA1	-0.75		SIN3A
SKA2	-0.75	E2F4	SIN3A
GTSE1	-0.75		SIN3A
DBF4	-0.74		SIN3A
SMC4	-0.74	E2F4	SIN3A
KIF4A	-0.74	E2F4	SIN3A
SGO1	-0.73		
CCNB1	-0.73		SIN3A
RBM47	-0.73	E2F4	SIN3A
PSMC3IP	-0.73	E2F4	SIN3A
HIST1H2AM	-0.73	E2F4	SIN3A
PRR5L	-0.72	E2F4	SIN3A
MIS18A	-0.72		
E2F8	-0.72	E2F4	SIN3A
DEPDC1B	-0.72	E2F4	SIN3A
ERI1	-0.72	E2F4	SIN3A
SLC43A3	-0.72	E2F4	
ATAD5	-0.71	E2F4	SIN3A
CDT1	-0.71	E2F4	SIN3A
MCM5	-0.71	E2F4	SIN3A
HIST1H1E	-0.71	E2F4	SIN3A
SFXN1	-0.71	E2F4	
C1orf112	-0.71	E2F4	SIN3A
INCENP	-0.71	E2F4	SIN3A
RACGAP1	-0.71	E2F4	SIN3A
TRAIP	-0.71	E2F4	SIN3A
DBF4B	-0.70		SIN3A
CEP72	-0.70		
GINS2	-0.70	E2F4	
ORC6	-0.70	E2F4	SIN3A

Supplementary table 3.

Up-regulated genes top 5 GO biological processes

pathway ID	pathway description	count in gene set	false discovery rate
GO:0007155	cell adhesion	24	0.000647
GO:0010942	positive regulation of cell death	19	0.000647
GO:0043068	positive regulation of programmed cell death	18	0.000647
GO:0043065	positive regulation of apoptotic process	17	0.0023
GO:0042981	regulation of apoptotic process	27	0.0048

Down-regulated genes top 5 GO biological processes

pathway ID	pathway description	count in gene set	false discovery rate
GO:0007049	cell cycle	44	2.24E-32
GO:0000278	mitotic cell cycle	36	5.08E-29
GO:1903047	mitotic cell cycle process	34	6.14E-28
GO:0022402	cell cycle process	37	2.68E-27
GO:0007067	mitotic nuclear division	22	1.77E-19

Supplementary table 4.

Primer name	Sequence
CYFIP2 F	CAGCCCAACCGAGTAGAGAT
CYFIP2 R	CTTCACCTCGCTGCAGAAC
PTCHD4 F	TATTTTGCTCCAGGCTGAGG
PTCHD4 R	ATGGCTCTGGCTGACTTGAC
PIK3IP1 F	TGGTGATCATCATTGCCATC
PIK3IP1 R	GCTGCATCTCCCTCTCACAT
p21 F	AGCAGAGGAAGACCATGTGGA
p21 R	AATCTGTCATGCTGGTCTGCC
exo1 F	AAGCGGGAATTGTGCAAG
exo1 R	TGAATACATCCCCAAGCTGTC
KIF23 F	TGCTGCCATGAAGTCAGCGAGAG
KIF23 R	CCA GTGGGCGCACCCTACAG
MXD4 F	GAGCTGAACTCCCTGCTGAT
MXD4 R	TTTTCTCCCTGGCGAAGTC
HAS2 F	TTCAGAGCACTGGGACGAAG
HAS2 R	GACATCTCCCCCAACACCTC
E2F7 F	AAGAGCGAGGTCGTAAACCA
E2F7 R	CCAGCTTCTGTTTTGCACAG
mcm10 F	TCTTATTTGGAGAAGTTCACAAAGC
mcm10 R	AGGTCAAGAGCTTCACCCATAA
MAD2L1 F	AAGTGGTGAGGTCCTGGAAA
MAD2l1 R	TTCCAACAGTGGCAGAAATG
CAPNS1 F	ATGGTTTTGGCATTGACACATG
CAPNS1 R	GCTTGCCTGTGGTGTCGC
SRPR F	CATTGCTTTTGCACGTAACCAA
SRPR R	ATTGTCTTGCATGCGGCC

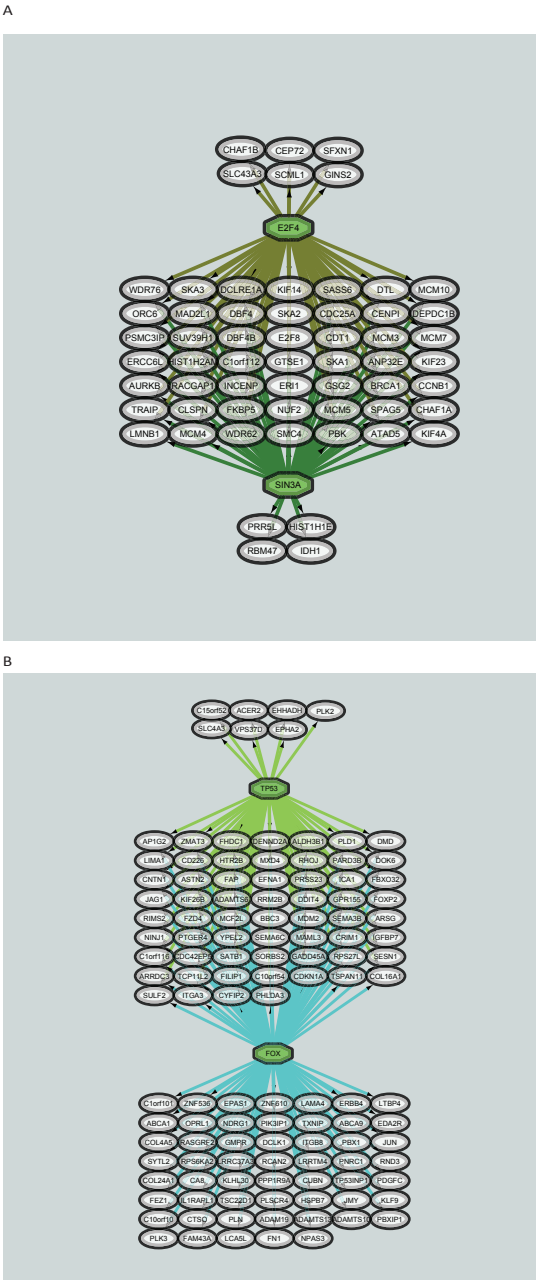

Supplementary figure 1. Gene regulatory network of genes transcriptionally affected upon MDMX knockdown. A) Gene regulatory network of genes downregulated upon MDMX depletion identifying the two major regulators E2F4 and SIN3A. B) Gene regulatory network of genes upregulated upon MDMX depletion identifying the two major regulators p53 and Forkhead box (FOX) transcription regulators.

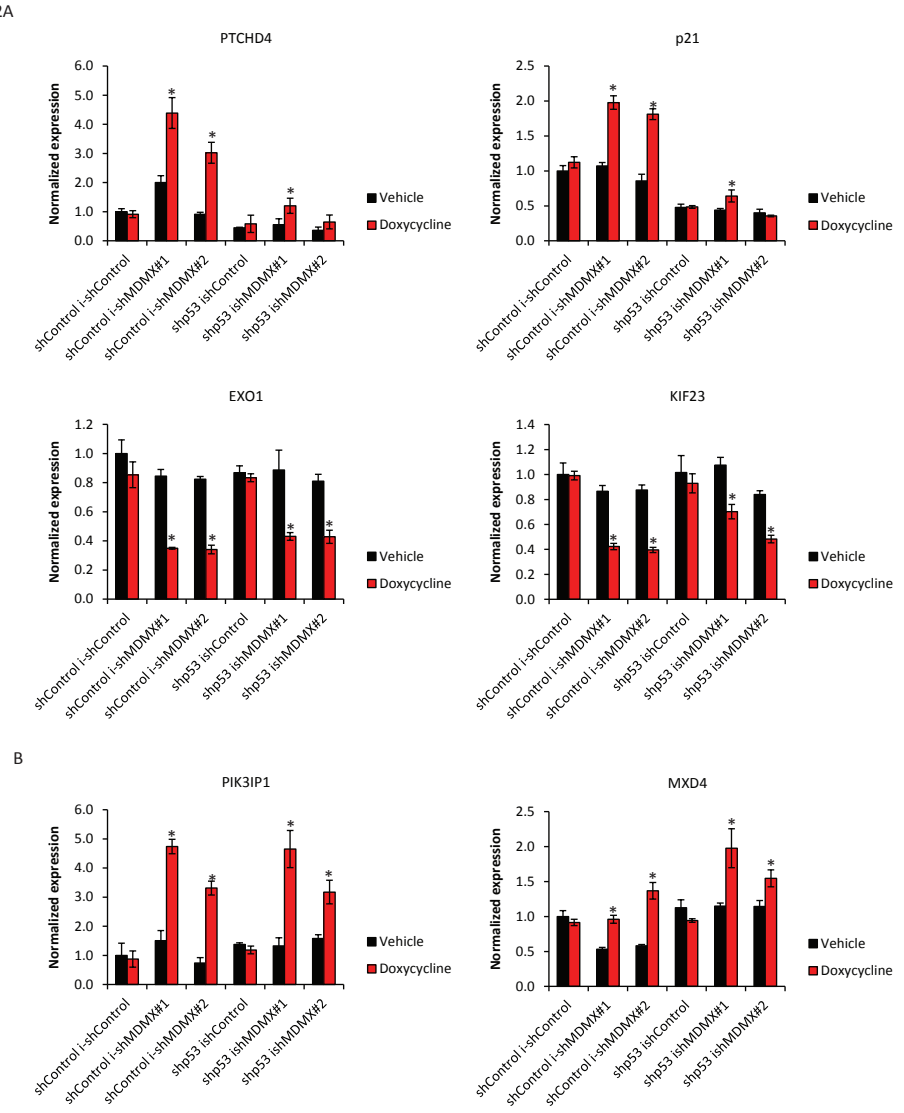

Supplementary figure 2. Transcriptional effects upon MDMX depletion in 92.1 cells. A) Relative mRNA expression of the downregulated genes EXO1 and KIF23, and the upregulated genes p21 and PTCHD4 upon MDMX depletion in 92.1/shCtrl and 92.1/shp53 cells. B) Relative mRNA expression of PIK3IP1 and MXD4 in 92.1 cells under conditions described in A. Significant differences in expression between vehicle and doxycycline treated cells are indicated with an asterisk (*).

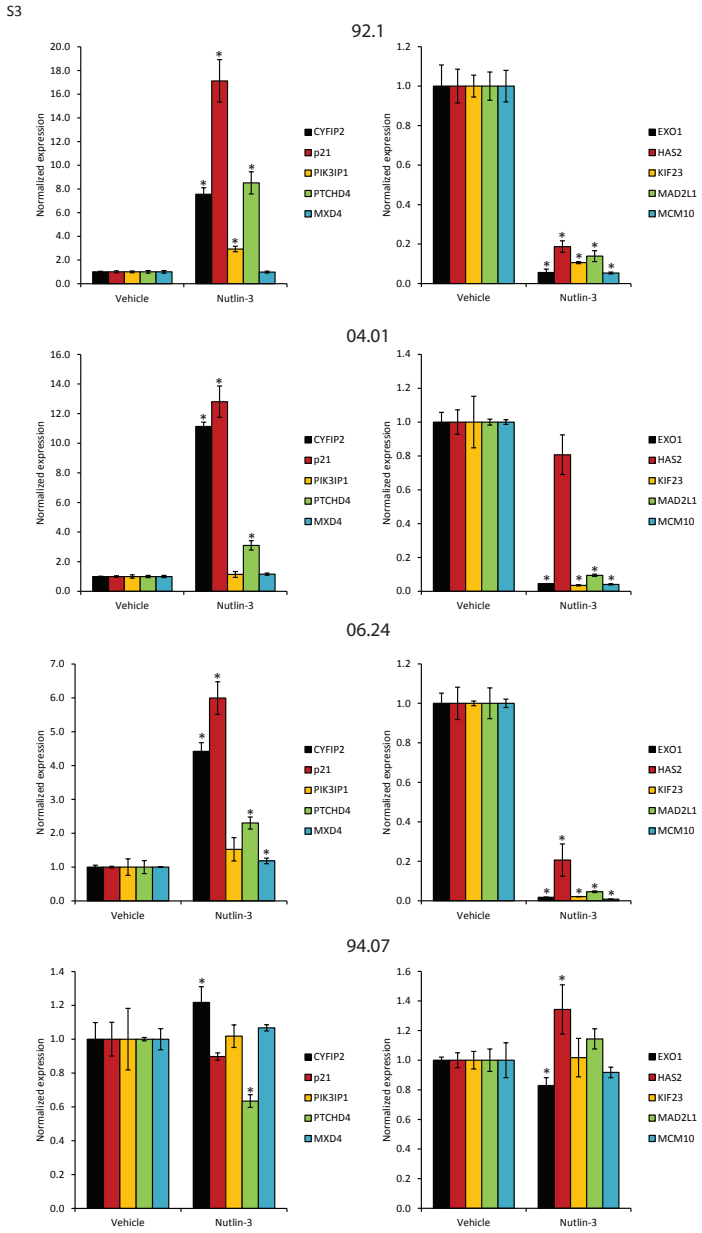

Supplementary figure 3. Effects of Nutlin-3 treatment on expression of 'MDMX target genes' in uveal and cutaneous melanoma cell lines. Relative mRNA expression of CYFIP2, p21, PIK3IP1, PTCHD4, MXD4, EXO1, HAS2, KIF23, MAD2L1 and MCM10 upon 24 hours of Nutlin-3 treatment in uveal melanoma cell line 92.1 and cutaneous melanoma cell lines 04.01, 06.24 and 94.07. Differences in expression between vehicle and Nultin-3 treated cells found to be significant are indicated with an asterisk (*).

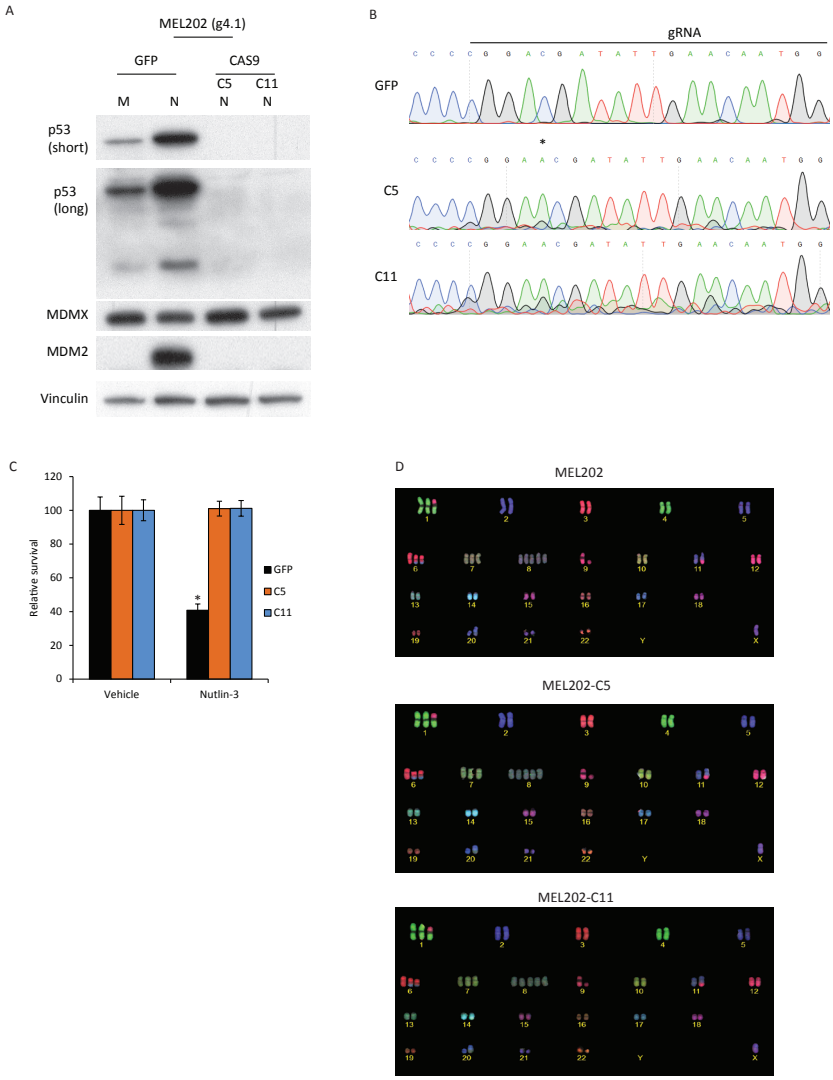

Supplementary figure 4. Generation of p53 knock-out MEL202 cells. A) Analysis of protein expression of MEL202 control cells and two distinct MEL202 p53 knockout cells treated for 24 hrs with DMSO (D) or 4 µM Nutlin-3 (N). The p53 protein levels increased in the GFP control cells upon Nutlin-3 treatment, but remained undetectable in the p53 knockout cells. MDMX levels showed minor differences between clones. MDM2 levels increased upon Nutlin-3 treatment in the p53 knockout cells but remained undetectable in the p53 KO cells. B) Sanger sequencing of control and p53 knockout clones. Shown are the guide RNA sequence and the insertion of one adenine, highlighted by the asterisk (*). C) Relative survival of MEL202 control- and MEL202 p53 KO cells upon 4 µM Nutlin-3 treatment for 72 hrs. Significant differences in relative survival between vehicle and Nutlin-3 treatment are indicated with an asterisk (*). D) COBRA-FISH analysis of chromosomal content of MEL202 control - and two distinct p53 knockout clones.

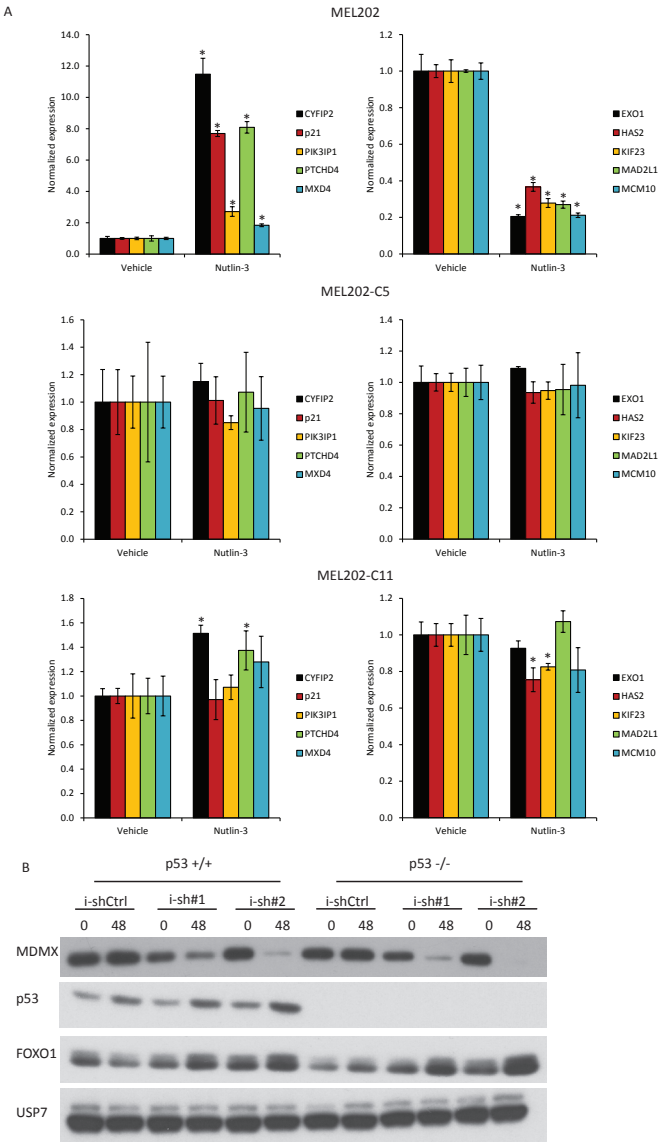

Supplementary figure 5. Effects of Nutlin-3 treatment on expression of 'MDMX target genes' in MEL202 control- and p53 knockout cells. A) Relative expression of EXO1, HAS2, KIF23, MAD2L1, MCM10, CYFIP2, p21, PTCHD4, PIK3IP1 and MXD4 in MEL202 control- and p53 knockout cells upon 24 hours of 4 µM Nutlin-3. Significant differences in expression between vehicle and Nutlin-3 treated cells are indicated with an asterisk (*). B) Protein expression analysis upon MDMX knockdown (48 hrs doxycycline, 10 ng/ml) in MEL202 control- and p53 knockout cells. The cells containing the distinct MDMX targeting shRNA constructs show a clear reduction of MDMX protein upon doxycycline treatment. MDMX depletion results in a slight increase of p53 and FOXO1 protein levels. USP7 was analysed to show equal loading.

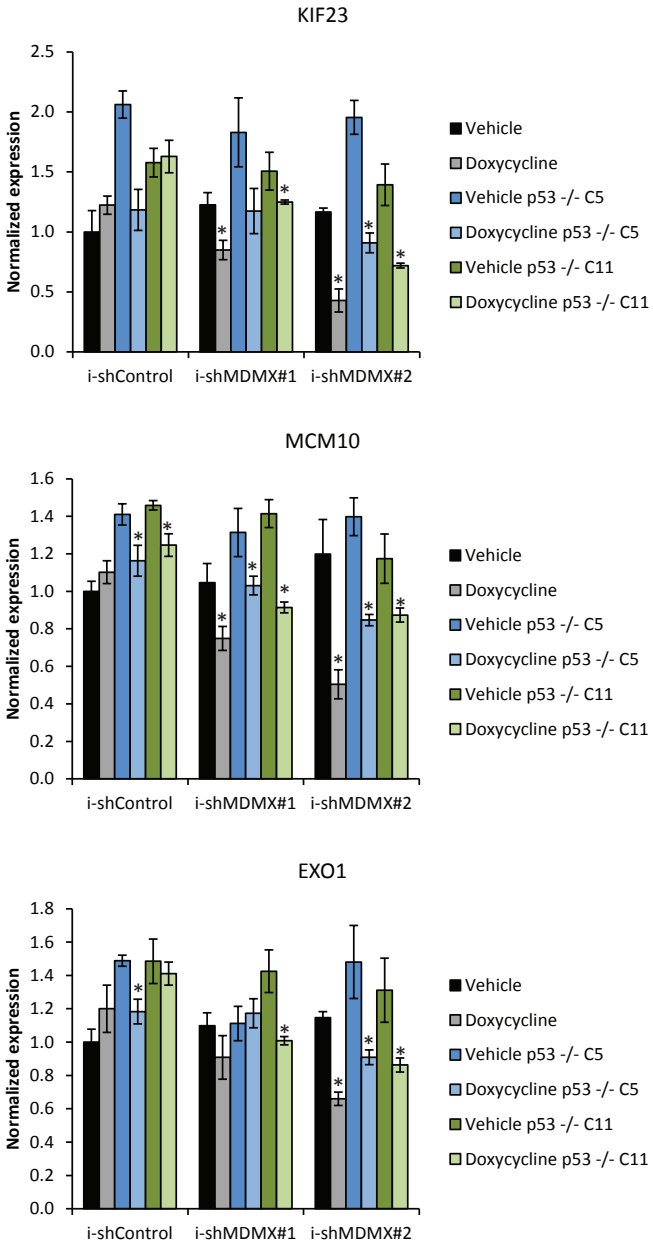

Supplementary figure 6. Repressing of transcription upon MDMX depletion is partly p53-independent. Relative mRNA expression of KIF23, MCM10 and EXO1 upon MDMX depletion (48 hour of 20 ng/ml doxycycline), in MEL202 control cells and MEL202 p53 knockout cells. Significant differences in expression between vehicle and doxycycline incubated samples is indicated with an asterisk (*).